LWT - Food Science and Technology 204 (2024) 116452

Contents lists available at ScienceDirect

LWT

journal homepage: www.elsevier.com/locate/lwt

Drying kinetics and water adsorption properties of jalapeño pepper seeds (*Capsicum annuum* L.): A study aiming at their recovery and integral exploitation

André Luiz Borges-Machado [a,*], Marcio Augusto Ribeiro-Sanches [a], Maria Júlia Neves Martins [a], Mario Luna-Flores [b,c], Guadalupe Luna-Solano [c], Silvio José Ferreira de Souza [a], Javier Telis-Romero [a]

[a] *Food Engineering and Technology Department, State University of São Paulo, São José Do Rio Preto, São Paulo, 15.054-000, Brazil*
[b] *Departamento de Ingeniería en Procesos Bioalimentarios, Universidad Tecnológica Del Centro de Veracruz, Cuitláhuac, Veracruz, Mexico*
[c] *Division of Postgraduate Studies and Research, Technological Institute of Orizaba, Orizaba, Mexico*

ARTICLE INFO

Keywords:
By-products
Equilibrium moisture content
Mathematical modeling
Sorption heat
Water activity

ABSTRACT

Drying kinetics (DK) and water adsorption isotherms (WAI) of Jalapeño pepper seeds (JPS) were evaluated and modeled at different temperatures. The proximate composition, flavonoid content (FC), and total phenolic compounds (TPC) of JPS were determined. Furthermore, JPS oil was extracted and characterized. Five mathematical models were tested to describe the JPS drying kinetics at five temperatures (40–80 °C) as well as the effective diffusion coefficient (D_{eff}) and activation energy (E_a) were calculated. The WAI of the JPS was determined at nine temperatures (8–72 °C) and five mathematical models were fitted to JPS adsorption data. Thermodynamic properties were also estimated. The JPS presented TPC (30.9 mg GAE/g), FC (17.4 mg catechin equivalents/g), fibers (54.8 g/100 d.b.), lipids (22.2 g/100 d.b.), and proteins (15.5 g/100 d.b.). The study on drying kinetics pointed out that the Weibull model best fitted to drying kinetics data, D_{eff} increased directly to temperature, and the E_a = 30.302 kJ/mol. The GAB model presented good accuracy in describing the WAIs that were classified as BET Type II. The net isosteric heat of adsorption and differential entropy decreased with increasing EMC. Enthalpy-entropy compensation theory was corroborated and characterized the adsorption of JPS as enthalpy-driven and spontaneous.

1. Introduction

Currently, in the agro-industrial sector, the trend is to recover and use all industrial by-products generated, aiming for sustainable food production, in line with efforts to reduce carbon emissions to zero (Valdez-Morales et al., 2021). The jalapeño pepper (*Capsicum annuum* L.) stands out as a crop of notable global importance due to its culinary and industrial versatility (Moreno-Escamilla et al., 2015). Approximately.

20 % of pepper is consumed in its natural form and 60 % of production is destined for processed products such as spices, canned products, and sauces (Nip, 2005; Sandoval-Castro et al., 2017). After processing, the jalapeño pepper by-product is a mixture of 95 % seeds and 5 % of peels, stalks, and unused pulp (Valdez-Morales et al., 2021) that are generated at different stages of industrial processing.

Jalapeño pepper seeds are sources of fiber (≃ 43 %, d.b.), proteins (≃ 20 %, d.b.), and lipids (≃ 17 %, d.b.) (Sandoval-Castro et al., 2014, 2017). Their high content of fibers demonstrates the potential of these seeds to be recovered and incorporated as ingredients in processed foods (Bouaziz et al., 2020; Garcia et al., 2020). The protein content appears to be recoverable, which is consistent with global trends toward the utilization of plant-based proteins as an excellent nutritious source for the human diet (Sá et al., 2020). Azabou et al. (2017) presented the high added value of red pepper seeds (*Capsicum annum*) owing to their chemical composition, including dietary fiber, crude proteins, and crude oil at around 60.96 %, 18.30 %, and 11.04 %, respectively. Sandoval-Castro et al. (2017) analyzed the bioactive compounds and antioxidant activity of the by-product of Jalapeño pepper (*Capsicum annuum*) for potential food and non-food applications. The ethanolic extract (80 %) of the by-product exhibited similar levels of total phenolics

* Corresponding author.
E-mail address: albmrv@gmail.com (A.L. Borges-Machado).

https://doi.org/10.1016/j.lwt.2024.116452
Received 16 February 2024; Received in revised form 2 June 2024; Accepted 24 June 2024
Available online 5 July 2024

compared to fresh pepper, with notable compounds such as epicatechin, rutin, and catechin. The oxidative activity was lower for by-products compared to fresh pepper. However, the byproduct still stands out in terms of antioxidant capacity, thanks to its higher content compared to tomato by-products.

The nutraceutical characteristics of pepper seed oil have been increasingly studied (Chen et al., 2024; Chouaibi et al., 2019; Ma et al., 2019a; Sangroula et al., 2024). Jalapeño pepper seed oil is a source of important lipophilic nutraceuticals such as β-carotene, essential fatty acids, capsaicin, α-tocopherol, and dihydrocapsaicin (Lu et al., 2019; Ma et al., 2019b; Sandoval-Castro et al., 2017) and has a pleasant flavor similar to sunflower oil (Jarret et al., 2013). Additionally, the proportion of fatty acids found closely resembled that of soybean and palm oil, predominantly composed of polyunsaturated fatty acid, specifically linoleic acid (Azabou et al., 2017). Sharma et al. (2013) highlights the importance of the capsaicin component present in the oil due to its nutraceutical characteristics and its medicinal applications in the areas of dermatology, gastrointestinal health, obesity, and cancer treatment.

With all the benefits mentioned above, the development of new nutritional products with the addition of pepper flour or seed oil remains scarce in the literature. (Cvetković et al., 2022; Valdez-Morales et al., 2021) mentioned several potential products: chocolate spreads, breakfast sauces, bakery items, and soup thickeners.

Despite of this trend towards valuing agro-industrial residues and converting them into high-value products, there are few studies in the literature evaluating the processing conditions for their stabilization, making it difficult to size the required operations adequately and efficiently before this conversion. Due to the high cost of energy, one of the most difficult aspects of employing by-products is the necessity for drying. This unit operation aims to enhance the stability against oxidative and enzymatic processes, as well as microbial spoilage while also reduces mass and volume, thus, lowering storage and transportation costs for by-products (Polachini et al., 2016; Rosa et al., 2021).

Knowledge and modeling of the drying kinetics and water sorption properties of JPS are essential to understand the interaction of the water with the dry matter of Jalapeño pepper seeds, thus, enhancing the correct equipment sizing, control, and the drying and storage processes of this by-product. Thus, ensuring its integrity and availability for further applications. This is the first study to present data regarding the drying kinetics and the water adsorption properties of jalapeño pepper seeds (*Capsicum annuum* L.) aiming for their recovery and full use. Thus, the main objectives of this study were to determine and model the drying kinetics and water sorption properties of jalapeño pepper seeds (*Capsicum annuum* L.) under storage and drying conditions.

2. Material and methods

2.1. Raw material

Fresh jalapeño peppers (*Capsicum annuum* L.) were purchased at a local supermarket (São José do Rio Preto, SP, Brazil) and transported to the Physical Measurements Laboratory at Unesp (Campus São José do Rio Preto). The peppers were washed with distilled water and had their stalk removed. Then, the seeds were manually separated, placed in low-density polypropylene bags, and stored under refrigeration at 4 °C.

2.2. Characterization of jalapeño pepper seeds (JPS)

2.2.1. Proximate composition of JPS

Lipids were determined by Soxhlet following the Ai 3–75 method (AOCS, 2009). The determination of fiber, protein and ash contents were conducted following the (AOAC, 2007) methodologies. The total fiber content which is the sum of the insoluble and soluble fiber fractions was determined according to method 991.43 based on enzymatic removal of starch and protein for further separation into soluble and insoluble fiber fractions by centrifugation. The total nitrogen was determined by micro-Kjeldahl (method 981.10) and the conversion factor equal to 6.25 were used to calculate the protein content. Ash content was determined by incineration in a muffle furnace (method 923.03) at 550 °C until white ashes were obtained. Carbohydrates were obtained by difference.

2.2.2. Total phenolic compounds (TPC) and flavonoids content (FC) of JPS

Total phenolic compounds were determined using the spectrophotometric method and the absorbance was measured at a wavelength of 740 nm (Singleton et al., 1999). The calibration curve was constructed using gallic acid (Dinâmica, Brazil) as standard reagent and the results were presented in mg of gallic acid equivalent per 100 g of sample (mg GAE/100 g). The total flavonoid content was determined using the spectrophotometric method based on the protocol described by (Zhishen et al., 1999) using a methanolic $AlCl_3$ solution. Catechin was used as a reference flavonoid and the results were presented in mg of catechin equivalents per g of seed extract.

2.2.3. Extraction and physicochemical characterization of JPS oil

The preparation and extraction of oil from jalapeño pepper seeds were carried out following the protocol described by (Rosa et al., 2021). The dried seeds at 60 ± 2 °C were grounded in a rotary mill (model MA340, Marconi, Piracicaba, SP, Brazil) and sieved through a 30 mesh sieve to obtain a powder with particles lower than 595 μm in size. This step was done aiming to enhance the oil extraction of the seeds. Filter paper cartridges containing 10 g of JPS powder were put inside to perform oil extraction using petroleum ether (40–60 °C for 6 h) in a Soxhlet extractor as described by the Ai 3–75 method (AOCS, 2009). The solvent was removed from the oil at 60 °C under vacuum and stored in an amber glass bottle at −18 °C. The JPS oil was characterized and evaluated according to its iodine index (g of I_2/100 g) (Cd method 1–25), refractive index at 40 °C (Cc method 7–25), free fatty acids content (% in oleic acid w/w) (Ca 5a-40 method), peroxide value (mEq peroxide/kg) (Cd 8–53 method), acid value (mg KOH/g) and saponification matter (mg KOH/g) (method of Cd 3–25). The methods mentioned above are described in the official methods for oils of the American Oil Chemists' Society (AOCS, 2009). The unsaponifiable matter (%) was performed according to (Lozano et al., 1993).

2.3. Convective hot air drying of JPS

A pilot-scale convective dryer with a process control system operated with Fieldbus technology (SMAR Industrial Equipment Ltda., Sertãozinho, Brazil) was used to study the drying kinetics of JPS. The same equipment was previously used and described in previous studies (Nicoleti et al., 2007; Rosa et al., 2015, 2021). The JPS drying kinetics were carried out at temperatures of 40, 50, 60, 70, and 80 °C with a constant dry air speed of 1.3 m/s. At least 30 min were spent for the set points to the dryer reached permanent conditions and then, the samples were evenly put in the chamber as a thin layer (layer thickness: 8 ± 0.1 mm). Each experiment used weighed 200 ± 0.5 g. The initial moisture content of JPS was determined at the beginning of the experiment using vacuum oven drying (method 950.46) according to (AOAC, 2007) procedure. The moisture content at each time was calculated in dry basis (d.b.) using the weight loss and dry solid weight of JPS and drying experiment was finished when the sample achieved the equilibrium moisture content (EMC). The relative humidity (RH) was recorded at the end of each test to calculate the water activity (a_w) using the relationship $a_w = RH/100$. The Newton, Page, Henderson and Pabis, Logarithmic, and Weibull models (Equations (1)–(5)) were fitted to the drying kinetics experimental data.

$$MR = exp(-kt) \quad (1)$$

$$MR = exp(-kt^n) \quad (2)$$

$$MR = a \bullet exp(-kt) \quad (3)$$

$$MR = a \bullet exp(-kt) + c \quad (4)$$

$$MR = exp\left[-\left(\frac{t}{\alpha}\right)^{\beta}\right] \quad (5)$$

in which: a, c, n: model coefficients; k: drying constant; α: scale parameter (min); β: shape parameter; t: drying time (min). The drying rate (DR) for each temperature was also estimated using Equation (6).

$$DR = \frac{MC_{t_1} - MC_{t_2}}{t_2 - t_1} \quad (6)$$

where MC_{t_1} and MC_{t_2} are the moisture contents in kg/kg d.b. at drying times t_1 and t_2, respectively.

2.3.1. Effective diffusion coefficient (D_{eff}) and activation energy (E_a)

The coefficients at different temperatures were determined using the solutions of Fick's second law for flat slab proposed by Crank (1975) truncated in the twelfth term via nonlinear regression (Equation (7)). The activation energy (E_a) was determined by using the linearized form of the Arrhenius model (Equation (8)) aiming to assess the dependence of D_{eff} on temperature.

$$MR = \frac{8}{\pi^2}\sum_{n=0}^{\infty}\frac{1}{(2n+1)^2}exp\left(\frac{-(2n+1)^2\pi^2 D_{eff}t}{4l^2}\right) \quad (7)$$

$$D_{eff} = D_0 \ exp\left[\frac{E_a}{RT}\right] \quad (8)$$

in which, n is the number of terms of the series, t is the time, l is the half thickness of the slab, D_0 is the pre-exponential factor of the Arrhenius equation (m^2/s); T is the absolute air temperature (K) and R is the universal gas constant (8.314 J/mol/K).

2.4. Water adsorption isotherms of JPS

The water adsorption isotherms of Jalapeño pepper seeds were determined using the Spiess and Wolf (1983) static gravimetric method at seven temperatures that simulate storage conditions (8 °C, 16 °C, 24 °C, and 32 °C) and drying conditions (40 °C, 48 °C, 56 °C, 64 °C, and 72 °C). For this, eleven saline solutions saturated with different salts (LiBr, LiCl, LiI, $K_2C_2H_3O_2$, $MgCl_2$, $Mg(NO_3)_2$, NaBr, $NaNO_3$, NaCl, KBr, and KCl) were used and placed in glass desiccators. These saturated saline solutions were used to achieve a relative humidity range between 4.8 % and 92.1 %. Storage temperatures were simulated in a BOD chamber (MA415, Marconi, Piracicaba, Brazil), and drying temperatures were simulated in an oven (MA030, Marconi, Piracicaba, Brazil). The water activities (a_w) of saline solutions at different temperatures (Table S1) were prepared according to data correlations presented by Labuza (1963) and Martins et al. (2023). The GAB, Peleg, Oswin, Halsey and Henderson models (Equations (9)–(13)) were fitted to the adsorption experimental data.

$$EMC = \frac{X_m C k a_w}{(1 - k a_w)(1 + (C-1) k a_w)} \quad (9)$$

$$EMC = k_1 a_w^{n_1} + k_2 a_w^{n_2} \quad (10)$$

$$EMC = M\left(\frac{a_w}{1 - a_w}\right)^N \quad (11)$$

$$EMC = (-h_1 \ ln(a_w))^{-\frac{1}{h_2}} \quad (12)$$

$$EMC = \left(-\frac{ln(1 - a_w)}{H_1}\right)^{\frac{1}{H_2}} \quad (13)$$

in which: X_m represents the monolayer moisture content (kg of water/kg dry matter), C, k, k_1, n_1, k_2, n_2, M, N, h_1, h_2 H_1, and H_2 are constants of the models, EMC is the equilibrium moisture content, and a_w is the water activity.

2.4.1. Thermodynamic properties of JPS adsorption

The models that best fit the experimental data of the adsorption isotherms at nine temperatures were used to determine water activity at a given equilibrium humidity. The values of $ln(a_w)$ were plotted as a function of 1/T for each EMC to calculate the net isosteric heat of adsorption (q_{st}) or enthalpy of sorption and differential entropy (ΔS). The q_{st} is the amount of energy needed to adsorb the water molecules into the active sites of the food matrix. It can be used to evaluate the dependence of the adsorption phenomenon on temperature and be accessed through the angular coefficients of Equation (14) known as the Clausius-Clapeyron equation (Rizvi, 2014).

$$\left.\frac{\partial(\ln a_w)}{\partial\left(\frac{1}{T}\right)}\right|_{EMC} = -\frac{Q_{st} - \lambda}{R} = -\frac{q_{st}}{R} \quad (14)$$

The differential entropy (ΔS) is proportional to the number of available sorption sites at a given energy level being associated with attraction-repulsive forces in the system (Yogendrarajah et al., 2015). According to Tagnamas et al. (2021), the linear relationship between ΔS and q_{st} can be described by Equation (15). Moreover, the enthalpy-entropy mechanism can be assessed by Equation (16), again, by linear regression according to Leffler (1955).

$$(-\ln a_w)|_{EMC} = \frac{q_{st}}{RT} - \frac{\Delta S}{R} \quad (15)$$

$$q_{st} = T_B \Delta S + \Delta G_B \quad (16)$$

in which ΔG_B is the Gibb's free energy at the isokinetic temperature (T_B) obtained. The isokinetic temperature is the temperature at which all the reactions regarding sorption proceed at the same rate (Červenka et al., 2015). According to Krug et al. (1976a,)Krug et al. (1976b, the compensation theory is valid only if T_B differs from the harmonic mean temperature (T_{hm}), calculated by Equation (17). To evaluate if T_B is significant different from T_{hm}, Equation (17) was used to calculate an interval of confidence of 95 %.

$$T_{hm} = \frac{n}{\sum_{i=1}^{n}(1/T)} \quad (17)$$

$$T_B = T_B \pm t_{m-2;0.025}\sqrt{Var(T_B)} \quad (18)$$

in which n is the number of adsorption curves, m represents the number of data pairs (ΔH, ΔS) and t is the Student's t-value at 0.025.

2.5. Statistical analysis

The five drying models and five water sorption models were fitted to the drying kinetics and water adsorption experimental data using OriginPro 2022 software (OriginLab Corporation, Northampton, MA). The accuracy of the fittings was evaluated analyzing the coefficient of determination (R^2_{adj}) and reduced chi-square (χ^2) of each regression. A good fit presents R^2_{adj} close to one and χ^2 close to zero (Vega-Gálvez et al., 2010). Furthermore, Akaike information criteria (AIC) and Bayesian information criteria (BIC) were calculated by Equations (19) and (20) to select the most suitable model to represent the drying and adsorption curves (Akaike, 1974; Schwarz, 1978).

$$AIC = -2\log\mathscr{L}(\hat{\theta}) + 2p \quad (19)$$

$$BIC = -2\log \mathscr{L}(\widehat{\theta}) + p\ln(n) \tag{20}$$

where, n is the quantity of experimental points, p is the quantity of parameters of the model, and $\mathscr{L}(\widehat{\theta})$ is the value of the likelihood function considering the parameters of the obtained model. The AIC considers both the number of model parameters and the R^2_{adj}, but, as the AIC values decreases as the number of data points tend to infinity, thus, it is not a "consistent" information criterion and cannot ensure that the best model will be chosen (Wagenmakers & Farrell, 2004). When compared to the AIC, the BIC is considered to be a more "consistent" information criterion because it pursues a penalty term for the quantity of data points and a penalty term for the parameters (Schwarz, 1978). Better predictability of the models is indicated by the lowest values of AIC and BIC (Wolfinger, 1993).

3. Results and discussion

3.1. Chemical composition

The JPS presented in dry basis: total fibers (52.967 ± 0.574 % of insoluble fibers and 1.821 ± 0.066 % of soluble fibers); lipids (22.225 ± 0.393 %); proteins (15.497 ± 1.010 %); ashes (3.677 ± 0.502 %). The high total fiber content (mainly insoluble fiber) demonstrates the great potential of jalapeño pepper seeds to be recovered and incorporated as ingredients in processed foods (Bouaziz et al., 2020; Garcia et al., 2020), such as meat products, which are deficient in dietary fiber. Regarding lipid content, when considering ordinary oilseed crops such as soybeans (18–20 %) and corn (3.1–5.7 %) (O'Brien, 2009), the high lipid content of JPS may turn them economically feasible for industrial extraction thus indicating the JPS potential as source of edible oil. Protein content also appears to be viable for recovery, as peas contain 20–25 % of proteins (Lu et al., 2019); amaranth (*Amaranthum*) contains approximately 14.5 % proteins (López et al., 2018); and quinoa (*Chenopodium quinoa*) contains approximately 13 % proteins (Mattila et al., 2018). Some authors have studied the extraction and functional properties of proteins isolated from pepper seeds (*Capsicum annuum* L. var. Annuum) of other varieties (Li et al., 2018), showing the potential of pepper seeds as a source of protein, which meets global trends in food science and technology for the use of plant-based proteins as an excellent nutritional source for the human diet (Sá et al., 2020).

The seeds also presented total phenolic compounds (30.911 ± 2.021 mg of gallic acid equivalents/g of seed extract) and flavonoids (17.467 ± 1.605 mg of catechin equivalents/g of seed extract). Sora et al. (2015) studied the antioxidant activity of fruits and seeds of peppers of the genus *Capsicum* and reported that seed extracts exhibited higher antioxidant capacity than extracts of the pulps. This shows the potential of seeds for the extraction and application of antioxidant compounds as natural ingredients in products, aiming to replace synthetic additives as well as promising ingredients for "clean label" products.

3.2. Chemical characterization of jalapeño pepper seed (JPS) oil

Table 1 presents the results of chemical characterization of the oil extracted from the JPS. Azabou et al. (2017) studying the red pepper seed oil presented similar results. The iodine index is a parameter that measures the unsaturation of the oil. The JPS oil had an iodine index of 168.003 ± 1.791 (g I_2/100 g of oil) that was higher than those found in Arjan seed oil (*Amygdalus reuteri*) which was 100 ± 1.5 (g I_2/100 g of oil) and in *Amygdalus scoparia* seed oil which was 101 ± 1.7 (g I_2/100 g of oil) (Tavakoli et al., 2018), indicating a higher level of unsaturation of fatty acids present in JPS oil. The refractive index is characteristic for each type of oil, being related to the degree of unsaturation, number of double bonds, and conjugations. The JPS oil had a refractive index of 1.469 ± 0.007 which is similar to the refractive indexes of the corn, sunflower, and soybean oils (Jorge et al., 2005). The JPS oil also presented 0.452 ± 0.008 % of free fatty acids. This parameter is an indicator of the hydrolysis of triglycerides in edible oils and the higher this index, the greater the concentration of free fatty acids which promote the oxidation process, reducing their shelf-life (Tavakoli et al., 2018). Furthermore, JPS oil had a peroxide index of 2.304 ± 0.033 (mEq peroxide/kg) that is a sensitive indicator index that measures the initial oxidation state of an oil. Rosa et al. (2021) used the same extraction conditions for papaya seed oil (*Carica papaya* L.) and it presented a higher level of free fatty acids (1.26 ± 0.04 %) and a higher level of peroxides (5.36 ± 0.10 mEq peroxide/kg) when compared to JPS oil. JPS oil also presented an acid value of 0.597 ± 0.010 (mg KOH/g), a saponification index of 201.332 ± 2.845 (mg KOH/g oil), and an unsaponifiable matter of 0.907 ± 0.039 %, similar to those reported for extra virgin olive oil (Tavakoli et al., 2018) emphasizing its high quality. The phenolic and flavonoid compounds present in JPS oil contributes to its high quality because these compounds are important natural antioxidant and have been associated with the oxidative stability of edible oils (Hashemi et al., 2017).

Table 1
Chemical characteristics of jalapeño pepper seeds (JPS) oil.

Quality parameter	Values[a]
Iodine index (g I_2/100 g of oil)	168.003 ± 1.791
Refractive index (40 °C)	1.469 ± 0.007
Free fat acids (%)	0.452 ± 0.008
Peroxide index (mEq peroxide/kg)	2.304 ± 0.033
Acid index (mg KOH/g oil)	0.597 ± 0.010
Saponification index (mg KOH/g oil)	201.332 ± 2.845
Unsaponifiable matter (%)	0.907 ± 0.039

[a] Mean value ± standard deviation.

3.3. Drying curves of JPS and kinetics modeling

The chemical composition highlighted above not only reveals promising opportunities for its use, but also demonstrates the easily degradable nature of JPS. The chemical and physical instability due to components susceptible to degradation highlights the need for the drying process as an essential step for their stabilization. Preserving the integrity of JPS is crucial to maximizing their appreciation potential before any attempt is made to convert them into value-added products. Fig. 1a presents the moisture ratio curves as a function of time for JPS, with an initial moisture content equal to 9.721 g/100 g w.b. at the temperatures studied (40 °C, 50 °C, 60 °C, 70 °C, and 80 °C). As expected, the greatest water loss occurred in the initial stages of drying and the moisture content of the samples drastically decreased with increasing drying time. This behavior demonstrates that mass transfer was greater in the initial drying periods. It was noted that after 768 min (12.8 h) of drying, the moisture contents of the samples at 40 °C, 50 °C, 60 °C, 70 °C and 80 °C were equal to 4.743, 3.933, 2.773, 2.280, and 1.843 g/100 g w.b., respectively, showing that drying time is reduced for about 2.5 times when doubling the drying temperature. The plots of the drying rates (DR) at the five studied temperatures as a function of the moisture content of JPS are presented in Fig. 1b. At high moisture contents, the DRs are higher than at medium and low moisture contents. The drying rate decreasing from the beginning to the end of the drying process indicates the absence of a constant rate period or the presence of a constant rate for a brief period in comparison to the whole drying process (Keneni et al., 2019), thus, an indicative of diffusion as the main phenomenon of the process.

Table 2 shows the coefficients and the fitting parameters of the models adjusted to the experimental data of drying. The Weibull and Page models presented the highest R^2_{adj} and χ^2 lowest when compared to the other models, at all the temperatures studied. The AIC and BIC values of the Weibull model were lower than those calculated for Page, thus, the Weibull model was selected to describe the drying curves of

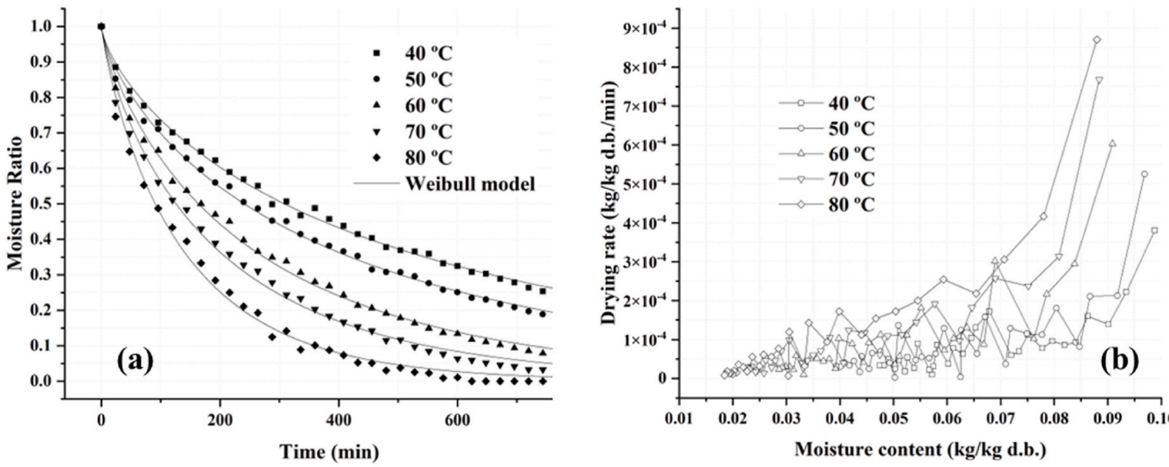

Fig. 1. Comparison between the experimental moisture ratios of Jalapeño pepper seeds and those predicted by the Weibull model at different temperatures.

Table 2
Coefficients and fitting parameters of the models applied to the drying kinetics data of JPS.

Model	Parameters	Temperature (°C)				
		40	50	60	70	80
Newton	$k•10^3$	2.070	2.550	3.720	4.790	6.920
	R^2_{aj}	0.9451	0.9550	0.9756	0.9782	0.9877
	$\chi^2 • 10^5$	215	207	142	134	78.0899
	AIC	−199.269	−200.540	−212.892	−214.932	−232.733
	BIC	−196.676	−197.947	−210.299	−212.339	−230.140
Page	$k•10^3$	10.580	11.46	11.4	13.48	13.51
	n	0.730	0.748	0.806	0.815	0.873
	R^2_{aj}	0.9968	0.9971	0.9955	0.9941	0.9929
	$\chi^2 • 10^5$	12.416	13.339	26.228	36.134	45.112
	AIC	−292.037	−289.670	−267.357	−256.800	−249.469
	BIC	−288.375	−286.008	−263.695	−253.138	−245.807
Henderson and Pabis	a	0.898	0.893	0.905	0.903	0.931
	$k•10^3$	1.770	2.210	3.330	4.300	6.430
	R^2_{aj}	0.9837	0.9871	0.9914	0.9911	0.9925
	$\chi^2 • 10^5$	63.923	59.655	50.501	54.804	48.031
	AIC	−237.959	−240.239	−245.736	−243.038	−247.391
	BIC	−234.297	−236.577	−242.074	−239.376	−243.729
Logarithmic	a	0.766	0.811	0.886	0.899	0.934
	$k•10^3$	2.700	3.000	3.670	4.410	6.230
	$c•10^3$	167.980	114.400	32.130	7.790	−8.470
	R^2_{aj}	0.9908	0.9922	0.9921	0.9909	0.9925
	$\chi^2 • 10^5$	35.992	35.872	46.382	55.971	47.637
	AIC	−255.395	−255.505	−247.025	−240.824	−246.144
	BIC	−250.837	−250.948	−242.468	−236.266	−241.587
Weibull	α	510.081	393.376	258.065	197.571	138.547
	β	0.730	0.749	0.807	0.817	0.875
	R^2_{aj}	0.9968	0.9971	0.9955	0.9941	0.9929
	$\chi^2 • 10^5$	12.415	13.337	26.221	36.116	45.099
	AIC	−292.039	−289.674	−267.366	−256.800	−249.470
	BIC	−288.377	−286.012	−263.704	−253.138	−245.808

JPS. This model was also used to describe the drying kinetics of peanut (Xie et al., 2022), red kidney bean (Doymaz, 2016), and pomegranate seeds (Doymaz, 2012). The scale (α) and shape (β) parameters of the Weibull model were both influenced by the temperature (Table 4). The α is the time required to complete approximately 63 % of the process (Corzo et al., 2008) and it reduced from 510.081 min at 40 °C to 138.547 min at 80 °C evidencing that loss of moisture at the beginning of the drying process is faster when increasing temperature. In contrast, β increased from 0.730 at 40 °C to 0.875 at 80 °C though being little affected by temperature. Corzo et al. (2008) reported that different values of β resulted in very different curves and could therefore describe several mechanisms such as convection, diffusion, and relaxation. Moreover, all the drying process happened under falling rate phase, which may have affected the values of the shape parameter.

3.3.1. *Moisture diffusivity and activation energy*

The solution of the second Fick's law for flat slab (l = 4 mm) with twelve terms was used to estimate the effective moisture coefficients (D_{eff}) through non-linear regression. In Table 3 are presented the D_{eff} and R^2_{adj} at each studied temperature. The model showed good accuracy to the experimental data ($R^2_{adj} > 0.995$) at all temperatures and D_{eff} rose directly with temperature from $1.648•10^{-10}$ to $6.103•10^{-10}$ m^2/s, which is typical of foodstuff (Kamal et al., 2020; Perea-Flores et al., 2012; D. Zhang et al., 2023). The influence of temperature on D_{eff} can be related to the quick migration of water molecules to the JPS surface due to the elevation of its internal vapor pressure which also increases

Table 3
Calculated effective diffusion coefficient and adjusted coefficient of determination of the linear regression at different temperatures of drying.

Temperature (°C)	D_{eff} (m^2/s)	R^2_{adj}
40	$1.648 \bullet 10^{-10}$	0.9971
50	$2.108 \bullet 10^{-10}$	0.9985
60	$3.201 \bullet 10^{-10}$	0.9977
70	$4.173 \bullet 10^{-10}$	0.9981
80	$6.103 \bullet 10^{-10}$	0.9950

directly with the temperature (Zhao et al., 2019). The activation energy (E_a) is a measure of the D_{eff} sensitivity regarding temperature as well as represents the minimum amount of energy to start moisture diffusion (Afolabi & Tunde-Akintunde, 2014) in JPS. The slope and intercept of the line resulted when plotted ln(D_{eff}) versus 1/T ($R^2_{aj} > 0.9879$) were used to calculate the pre-exponential factor of Arrhenius (D_0) and the E_a being equal to $1.778 \bullet 10^{-5}$ m^2/s and 30.302 kJ/mol, respectively. The E_a of JPS was close to the ones reported for *Jatropha curcas* L. seeds (Keneni et al., 2019) and Hass avocado seeds (Avhad & Marchetti, 2016).

Table 4
Coefficients and fitting parameters of the models applied to the adsorption data of JPS.

Model		Temperature (°C)								
		8	16	24	32	40	48	56	64	72
GAB	X_m	0.083	0.078	0.058	0.055	0.050	0.049	0.046	0.045	0.039
	C	7.439	7.483	8.842	8.937	9.010	8.799	8.309	9.678	7.129
	k	0.680	0.640	0.725	0.711	0.719	0.707	0.706	0.7688	0.6856
	R^2_{aj}	0.9981	0.9974	0.9971	0.9973	0.9883	0.9920	0.9982	0.9928	0.9947
	$\chi^2 \bullet 10^5$	0.770	0.660	0.595	0.428	1.447	0.839	0.161	0.161	0.567
	AIC	−118.348	−120.050	−121.189	−135.390	−111.415	−117.410	−135.560	−127.391	−126.350
	BIC	−123.423	−125.125	−126.264	−140.465	−116.490	−122.485	−140.635	−132.467	−131.425
Peleg	k_1	0.144	0.140	0.102	0.117	0.113	0.093	0.084	0.074	0.029
	n_1	0.642	0.689	0.589	0.697	0.734	0.642	0.631	0.593	0.338
	k_2	0.093	0.058	0.085	0.062	1.715	0.056	0.050	0.062	0.080
	n_2	3.678	4.390	3.463	5.402	21.412	4.091	3.277	3.387	1.349
	R^2_{aj}	0.9985	0.9976	0.9973	0.9991	0.9901	0.9912	0.9989	0.9956	0.9973
	$\chi^2 \bullet 10^5$	0.610	0.625	0.550	0.151	1.228	0.922	0.103	0.350	0.191
	AIC	−115.046	−114.781	−116.183	−130.445	−111.415	−117.410	−135.560	−127.391	−126.350
	BIC	−125.057	−124.792	−126.194	−140.456	−116.490	−122.485	−140.635	−132.467	−131.425
Oswin	M	0.095	0.083	0.073	0.069	0.062	0.060	0.056	0.053	0.051
	N	0.349	0.364	0.401	0.404	0.416	0.420	0.431	0.444	0.451
	R^2_{aj}	0.9665	0.9747	0.9876	0.9881	0.9851	0.9874	0.9935	0.9947	0.9894
	$\chi^2 \bullet 10^5$	13.293	6.499	2.509	1.897	1.842	1.330	0.586	0.418	0.750
	AIC	−90.961	−98.833	−109.303	−112.380	−112.704	−116.283	−125.303	−129.024	−122.581
	BIC	−93.196	−101.068	−111.538	−114.615	−114.939	−118.518	−127.538	−131.259	−124.816
Halsey	$H_1 \bullet 10^3$	2.930	3.330	4.860	5.08	5.500	5.780	6.280	7.040	7.270
	H_2	2.278	2.097	1.852	1.791	1.700	1.660	1.597	1.531	1.499
	R^2_{aj}	0.9174	0.9319	0.9583	0.9570	0.9610	0.9624	0.9690	0.9756	0.9634
	$\chi^2 \bullet 10^5$	32.735	17.519	8.416	6.844	4.825	3.958	2.790	1.919	2.581
	AIC	−81.048	−87.925	−95.989	−98.264	−102.109	−104.289	−108.134	−112.248	−108.990
	BIC	−83.283	−90.160	−98.224	−100.499	−104.344	−106.524	−110.369	−114.483	−111.225
Henderson	H_1	2.930	3.330	4.860	5.080	72.633	81.030	84.175	84.184	86.547
	H_2	0.003	0.003	0.005	0.005	1.710	1.723	1.698	1.666	1.649
	R^2_{aj}	0.9978	0.9976	0.9968	0.9991	0.9898	0.9932	0.9993	0.9959	0.9967
	$\chi^2 \bullet 10^5$	0.982	0.689	0.711	0.159	1.266	0.715	0.067	0.322	0.235
	AIC	−119.621	−123.522	−123.165	−139.654	−116.824	−123.111	−149.087	−131.899	−135.363
	BIC	−121.856	−125.757	−125.400	−141.889	−119.059	−125.346	−151.322	−134.134	−137.598

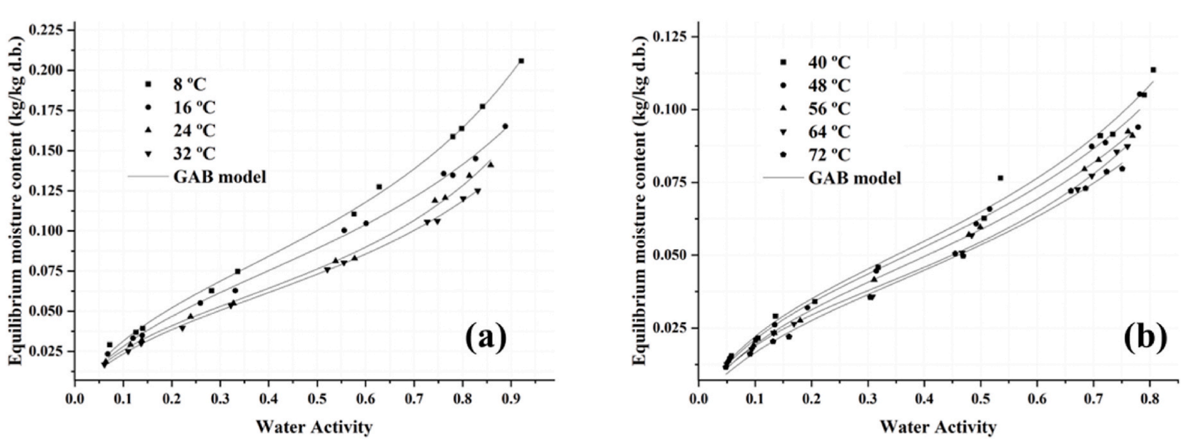

Fig. 2. Comparison between the experimental equilibrium moisture contents of Jalapeño pepper seeds and those predicted by the GAB model at storage (a) and drying (b) temperatures.

3.4. Water adsorption isotherms of JPS and modeling

As shown previously, the drying curves reinforce the importance of stabilizing the JPS before proceeding with any other recovery step. Therefore, the evaluation of sorption isotherms offers a better understanding of the moisture adsorption behavior of JPS under different temperature conditions, being important data for the correct design of the drying and storage process. Fig. 2 presents the variation of EMC as a function of the water activity of JPS at different storage (8 °C, 16 °C, 24 °C and 32 °C) and drying (40 °C, 48 °C, 56 °C 64 °C and 72 °C) temperatures. The EMC of JPS ranged from 0.0115 to 0.2058 kg/kg d.b. and the a_w varied from 0.048 to 0.921. These values were lower than the values found for papaya seeds (0.179–0.969 kg/kg d.b.) in a temperature range of 20–80 °C (Rosa et al., 2021). This fact may be related to the capsaicin present in JPS once that the sorption capacity of the food matrix is dependent on its structure and chemical composition (Arslan-Tontul, 2020). JPS have a high amount of capsaicin that are molecules whose chemical structure has a slightly polar character (Castro-Muñoz et al., 2022; Rezazadeh et al., 2022) that may probably make the water adsorption of JPS more difficult when compared to papaya seeds.

When analyzing the isotherms at constant temperature, it is noted that there was an increase in the EMC of the JPS due to the increase in water activity. In contrast, at the same water activity, increasing temperature reduced the EMC of JPS, showing that JPS became less hygroscopic with increasing sorption temperature, at constant a_w. The increase in temperature probably increased the kinetic energy and the water molecules excitation state which caused a reduction in the binding forces between the water molecules and the sorption sites, resulting in a loss of the EMC of the JPS to the environment (Al-Muhtaseb et al., 2002). Moreover, the impact of temperature on JPS adsorption isotherms is more pronounced at temperatures that simulate storage conditions (8, 16, 24, and 32 °C) when compared to drying conditions (48, 48, 56, 64, and 72 °C).

According to the classification by Brunauer et al. (1940), the adsorption isotherms of JPS (Fig. 2) can be classified as type II, due to its S or sigmoid shape. This sorption behavior has also been found in papaya (Rosa et al., 2021), chia (Arslan-Tontul, 2020), and melon (Mallek-Ayadi et al., 2020) seeds. Rosa et al. (2021) and Polachini et al. (2016) reported three regions in type II isotherms: the first region is associated with the monolayer moisture content (X_m) under conditions of $a_w \leq 0.3$ in which water molecules are strongly bounded to the food matrix, justifying the low moisture sorption in this region when compared to regions with higher a_w values; the second region is characterized by multilayer water, which shows an almost linear behavior and is at an a_w between 0.3 and 0.6; and the third region under conditions of $a_w \geq 0.6$ where the water molecules are weakly bounded to the JPS matrix and available for microbiological and chemical reactions.

The estimated coefficients and fitting parameters obtained from the adjustment of the mathematical models to the adsorption experimental data at storage and drying temperatures are shown in Table 4. The Halsey model showed the lowest R^2_{adj} and the highest χ^2, AIC, and BIC values, followed by the Oswin model. Hence, GAB, Peleg, and Henderson models showed a better fit. Comparing the BIC values of the GAB, Peleg, and Henderson models, it was observed that the Henderson model presented the lowest BIC values at six temperatures. The GAB model is the second-best model to represent the adsorption isotherms because it shows BIC values slightly higher than the Henderson model but lower than the other ones at six temperatures. Due to the physical meaning of the coefficients of the GAB model (X_m, C, and K), versatility when applied to food sorption, and mathematical simplicity when compared to Henderson model, the GAB model was chosen to describe the WAI of JPS as well as for thermodynamic properties estimations. The monolayer moisture content (X_m) is the quantity of water strongly adsorbed by active sites on the food surface and is recognized as a crucial factor in guaranteeing food stability (Kurozawa et al., 2015). The X_m decreased from 0.083 kg/kg d.b. at 8 °C to 0.039 kg/kg d.b. at 80 °C, and it can be associated with temperature rising. The water molecules become more activated with temperature increase causing an increase in the energy levels, destabilizing them that escape from the water binding sites of the JPS, resulting in a reduced monolayer moisture content (Zhang et al., 2022). These values, combined with the JPS drying curves, can be used to optimize the process, avoiding excessive energy expenditure without achieving adequate levels of moisture reduction.

3.4.1. Thermodynamic properties of JPS adsorption

Fig. 3a shows the net isosteric heat of adsorption (q_{st}) plotted as a function of an interval of EMC from 0.07 to 0.13 kg/kg d.b. It is noted that q_{st} exponentially increased from 4105 to 9588 J/mol with decreasing EMC suggesting that the energy required to bind water molecules to sorption sites was higher than the energy required to retain water molecules together in the liquid phase (Choudhury et al., 2011). It is worth noting that the moisture content at which the highest enthalpy and entropy values were achieved are very close to the monolayer moisture values estimated by the GAB model. This is due to the existence of highly active polar sites that bind water, incorporating water into the food matrix monolayer (Al-Mahasneh et al., 2012). Raw pinhão (Cladera-Olivera et al., 2008), whole chia (Arslan-Tontul, 2020), and papaya (Rosa et al., 2021) seeds presented similar results. The Riedel model showed a good fit to the calculated data ($R^2_{aj} = 0.9996$) and coefficients C_r and B_r equal to 22812.216 J/mol and 12.399, respectively (Fig. 3a). Differential entropy is proportional to the quantity of possible sorption sites at a given level of energy as well as the spatial configuration of the water and food matrix (Silva et al., 2021). The differential entropy (ΔS) reduced practically linearly from 24.990 to 13.352 kJ/mol/K with rising EMC (Fig. 3b), because as the sorption sites become occupied, there is a loss of rotational movement of water molecules, resulting in a drop in entropy and a rise in moisture content, hence, a system disorder (Kurozawa et al., 2015). The influence of EMC on ΔS can be described by a first-order polynomial in which the slope and the intercept are equal to −194.521 and 38.128, respectively.

A strong linear correlation was observed when plotting q_{st} against ΔS, indicating the existence of an enthalpy-entropy mechanism of compensation. Linear regression using Equation (15) were performed and provided a $R^2_{adj} = 0.9993$. The intercept of the line is equal to the Gibbs free energy, $\Delta G = -1189.20$ J/mol at the isokinetic temperature, this being equal to the slope, $T_B = 428.19$ K. The interval of confidence of 95 % for T_B proposed by (Krug et al., 1976a; Krug et al., 1976b) and the harmonic mean temperature were estimated at 11.35 and $T_{hm} = 311.78$ K, respectively. The negative sign of ΔG pointed out that the adsorption phenomenon was spontaneous. The T_β was higher than T_{hm} characterizing the adsorption process as enthalpy-driven (Spada et al., 2013). In addition, T_β is out of the interval of confidence, corroborating the existence of a compensation enthalpy-entropy mechanism.

4. Conclusion

The JPS are a source of insoluble fibers, lipids, proteins, antioxidant agents, and phenolic compounds, highlighting their potential as raw material for the development of value-added products. The JPS oil presented high levels of unsaturation of fatty acids and quality parameters comparable to olive oil. The drying experiments were conducted in the falling-rate period; thus, diffusion was the major mechanism of moisture transfer. The moisture loss of JPS can be best predicted by the Weibull model due to its great fit to the drying kinetics data. The effective diffusivity coefficient increased from $1.648 \bullet 10^{-10}$ to $6.103 \bullet 10^{-10}$ m^2/s with the drying temperature and hence the drying time decreased. The activation energy for moisture diffusion was equal to 30.302 kJ/mol. The adsorption isotherms of JPS presented a sigmoid shape and, thus, classified as BET Type II. The GAB and Henderson

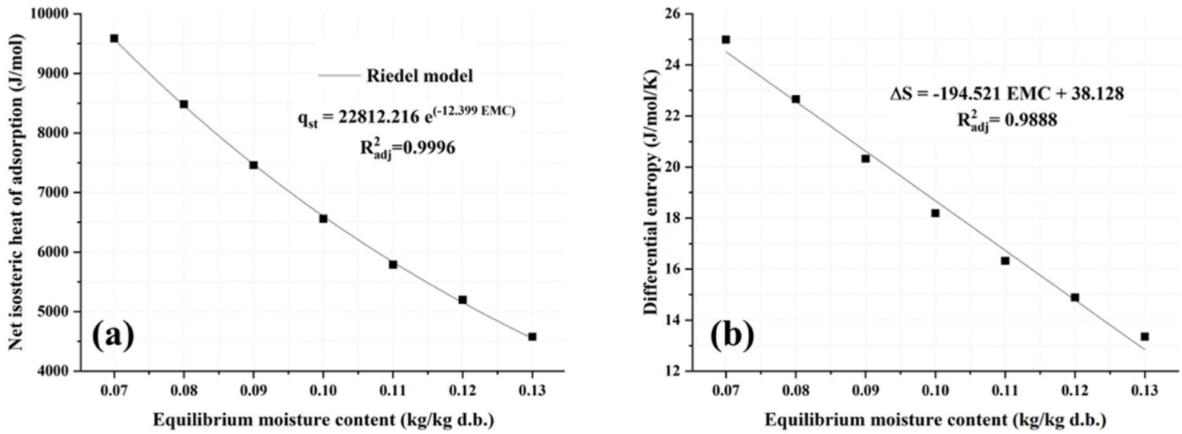

Fig. 3. Net isosteric heat of adsorption (a) and differential entropy (b) as function of equilibrium moisture content.

models are appropriate for describing the adsorption process. The net isosteric heat of adsorption exponentially increased from 3699.98 to 8482.77 kJ/mol with decreasing EMC. Similar behavior was observed in the ΔS which decreased almost linearly from 24.990 to 13.352 kJ/mol/K with rising EMC. The enthalpy-entropy compensation mechanism was validated and the provided information allowed us to characterize the adsorption as enthalpy-driven and spontaneous. All this data collected can contribute to extending the shelf life of jalapeño pepper seeds, targeting future industrial applications and contributing to sustainability and efficiency in the food and bioproducts industry.

CRediT authorship contribution statement

André Luiz Borges-Machado: Writing – review & editing, Writing – original draft, Methodology, Investigation, Formal analysis. **Marcio Augusto Ribeiro-Sanches:** Writing – review & editing, Methodology, Formal analysis. **Maria Júlia Neves Martins:** Writing – review & editing, Methodology, Formal analysis. **Mario Luna-Flores:** Writing – review & editing, Writing – original draft, Supervision, Resources, Methodology, Investigation. **Guadalupe Luna-Solano:** Writing – review & editing, Writing – original draft, Resources, Methodology, Investigation. **Silvio José Ferreira de Souza:** Writing – review & editing, Resources, Methodology, Investigation. **Javier Telis-Romero:** Writing – review & editing, Writing – original draft, Resources, Project administration, Methodology, Investigation, Formal analysis, Conceptualization.

Declaration of competing interest

The authors declare that they have no known competing financial interests or personal relationships that could have appeared to influence the work reported in this paper.

Data availability

Data will be made available on request.

Acknowledgments

The authors thank the Coordenação de Aperfeiçoamento de Pessoal de Nível Superior - Brasil (CAPES) - Finance Code 001 and the Conselho Nacional de Desenvolvimento Científico e Tecnológico (CNPq) - Award Number: 314459/2021-9.

NOMENCLATURE

JPS	Jalapeño pepper seed
MR	Moisture ratio
MC	Moisture content
DR	Drying rate
a, c, n	Drying models coefficients
k	drying constant
α	scale parameter
β	shape parameter
t	drying time
D_{eff}	Effective diffusion coefficient
E_a	activation energy
LiBr	Lithium bromide
LiCl	Lithium chloride
$MgCl_2$	Magnesium chloride
NaI	Sodium iodide
K_2CO_3	Potassium carbonate
$Mg(NO_3)_2$	Magnesium nitrate
NaBr	Sodium bromide
KI	Potassium iodide
NaCl	Sodium chloride
$(NH_4)_2SO_4$	Ammonium sulfate

KCl Potassium chloride
KNO_3 Potassium nitrate
K_2SO_4 Potassium sulfate
AIC Akaike information criterion
a_w Water activity
BIC Bayesian information criterion
C Constant of GAB model
GAB Guggenheim-Anderson-de Boer
h_1 and h_2 Constants of Halsey model
H_1 and H_2 Constants of Henderson model
k Constant of GAB model
k_1 and k_2 Constants of Peleg model
m Number of (ΔH, ΔS) data pairs
M and N Constants of Oswin model
n Number of isotherms
n_1 and n_2 Constants of Peleg model
C_r Isosteric heat of sorption at the first water molecule
B_r Constant of Riedel's model
Q_{st} Integral heat of sorption
q_{st} Net isosteric heat of sorption
R Universal gas constant (8.314 J/mol•K)
R^2_{adj} Adjusted coefficient of determination
RMSE Root mean square error
RH Relative humidity
T Temperature
T_B Isokinetic temperature
T_{hm} Harmonic mean temperature
EMC Equilibrium moisture content
X_m Monolayer moisture content
λ Heat vaporization of pure water
ΔG_B Free Gibbs energy at isokinetic temperature
$\overline{\Delta H}$ Average enthalpy
ΔH Differential enthalpy of sorption
$\overline{\Delta S}$ Average entropy
ΔS Differential entropy of sorption
χ^2 Reduced chi-square

Appendix A. Supplementary data

Supplementary data to this article can be found online at https://doi.org/10.1016/j.lwt.2024.116452.

References

Afolabi, T. J., & Tunde-Akintunde, T. Y. (2014). Effect of drying conditions on energy utilization during cocoyam drying. *Agricultural Engineering International: CIGR Journal, 16*(4), 135–145.

Akaike, H. (1974). A new look at the statistical model identification. *IEEE Transactions on Automatic Control, 19*(6), 716–723. https://doi.org/10.1109/TAC.1974.1100705

Al-Mahasneh, M. A., Bani Amer, M. M., & Rababah, T. M. (2012). Modeling moisture sorption isotherms in roasted green wheat using least square regression and neural-fuzzy techniques. *Food and Bioproducts Processing, 90*(2), 165–170. https://doi.org/10.1016/j.fbp.2011.02.007

Al-Muhtaseb, A. H., McMinn, W. A. M., & Magee, T. R. A. (2002). Moisture sorption isotherm characteristics of food products: A review. *Food and Bioproducts Processing: Transactions of the Institution of of Chemical Engineers, Part C, 80*(2), 118–128. https://doi.org/10.1205/09603080252938753

AOAC. (2007). Association of official analytical chemistry. In *Official methods of analysis to AOAC International* (18th ed.).

Arslan-Tontul, S. (2020). Moisture sorption isotherm, isosteric heat and adsorption surface area of whole chia seeds. *Lwt, 119*(October 2019), Article 108859. https://doi.org/10.1016/j.lwt.2019.108859

Avhad, M. R., & Marchetti, J. M. (2016). Mathematical modelling of the drying kinetics of Hass avocado seeds. *Industrial Crops and Products, 91*, 76–87. https://doi.org/10.1016/j.indcrop.2016.06.035

Azabou, S., Taheur, F. B., Jridi, M., Bouaziz, M., & Nasri, M. (2017). Discarded seeds from red pepper (Capsicum annum) processing industry as a sustainable source of high added-value compounds and edible oil. *Environmental Science and Pollution Research, 24*(28), 22196–22203. https://doi.org/10.1007/S11356-017-9857-9/FIGURES/3

Bouaziz, M. A., Bchir, B., Ben Salah, T., Mokni, A., Ben Hlima, H., Smaoui, S., Attia, H., & Besbes, S. (2020). Use of endemic date palm (phoenix dactylifera L.) seeds as an insoluble dietary fiber: Effect on Turkey meat quality. *Journal of Food Quality, 2020*. https://doi.org/10.1155/2020/8889272

Brunauer, S., Deming, L. S., Deming, W. E., & Teller, E. (1940). On the theory of the van der Waals adsorption of gases. *Journal of the American Chemical Society, 62*(7), 1723–1732.

Castro-Muñoz, R., Gontarek-Castro, E., & Jafari, S. M. (2022). Up-to-date strategies and future trends towards the extraction and purification of capsaicin: A comprehensive review. *Trends in Food Science & Technology, 123*, 161–171. https://doi.org/10.1016/J.TIFS.2022.03.014

Červenka, L., Hloušková, L., & Žabčíková, S. (2015). Moisture adsorption isotherms and thermodynamic properties of green and roasted Yerba mate (Ilex paraguariensis). *Food Bioscience, 12*, 122–127. https://doi.org/10.1016/j.fbio.2015.10.001

Chen, Y., Zhang, X., Liu, X., Liu, Y., Hou, A., Wang, Y., Li, L., Peng, X., & Xiao, Y. (2024). Discrimination and characterization of volatile organic compounds and nutritional values of three varieties of chopped pepper seeds. *Food Chemistry X, 21*, Article 101150. https://doi.org/10.1016/J.FOCHX.2024.101150

Chouaibi, M., Rezig, L., Hamdi, S., & Ferrari, G. (2019). Chemical characteristics and compositions of red pepper seed oils extracted by different methods. *Industrial Crops and Products, 128*, 363–370. https://doi.org/10.1016/J.INDCROP.2018.11.030

Choudhury, D., Sahu, J. K., & Sharma, G. D. (2011). Moisture sorption isotherms, heat of sorption and properties of sorbed water of raw bamboo (Dendrocalamus longispathus) shoots. *Industrial Crops and Products, 33*(1), 211–216. https://doi.org/10.1016/j.indcrop.2010.10.014

Cladera-Olivera, F., Pettermann, A. C., Noreña, C. P. Z., Wada, K., & Marczak, L. D. F. (2008). Thermodynamic properties of moisture desorption of raw pinhão (Araucaria angustifolia seeds). *International Journal of Food Science and Technology, 43*(5), 900–907. https://doi.org/10.1111/j.1365-2621.2007.01540.x

Corzo, O., Bracho, N., Pereira, A., & Vásquez, A. (2008). Weibull distribution for modeling air drying of coroba slices. *Lwt, 41*(10), 2023–2028. https://doi.org/10.1016/j.lwt.2008.01.002

Crank, J. (1975). The mathematics of diffusion. In *Journal of the American chemical society* (2nd ed.). Clarendon Press. https://doi.org/10.1021/ja01562a072.

Cvetković, T., Ranilović, J., & Jokić, S. (2022). Quality of pepper seed by-products: A review. *Foods, 11*, 748. https://doi.org/10.3390/FOODS11050748, 11(5), 748.

Doymaz, I. (2012). Drying of pomegranate seeds using infrared radiation. *Food Science and Biotechnology, 21*(5), 1269–1275. https://doi.org/10.1007/s10068-012-0167-1

Doymaz, İ. (2016). Hot-air drying and rehydration characteristics of red kidney bean seeds. *Chemical Engineering Communications, 203*(5), 599–608. https://doi.org/10.1080/00986445.2015.1056299

Garcia, M. V., Milani, M. S., & Ries, E. F. (2020). Production optimization of passion fruit peel flour and its incorporation into dietary food. *Food Science and Technology International, 26*(2), 132–139. https://doi.org/10.1177/1082013219870011

Hashemi, S. M. B., Mousavi Khaneghah, A., Koubaa, M., Lopez-Cervantes, J., Yousefabad, S. H. A., Hosseini, S. F., Karimi, M., Motazedian, A., & Asadifard, S. (2017). Novel edible oil sources: Microwave heating and chemical properties. *Food Research International, 92*, 147–153. https://doi.org/10.1016/j.foodres.2016.11.033

Jarret, R. L., Levy, I. J., Potter, T. L., & Cermak, S. C. (2013). Seed oil and fatty acid composition in Capsicum spp. *Journal of Food Composition and Analysis, 30*(2), 102–108. https://doi.org/10.1016/j.jfca.2013.02.005

Jorge, N., Bellei Prazeres Soares, B., & Martins Lunardi Cassia Roberta Malacrida, V. (2005). Alterações físico-químicas dos óleos de GIRASSOL, milho E soja em FRITURAS. *Quimica Nova, 28*(6), 947–951.

Kamal, M. M., Ali, M. R., Shishir, M. R. I., & Mondal, S. C. (2020). Thin-layer drying kinetics of yam slices, physicochemical, and functional attributes of yam flour. *Journal of Food Process Engineering, 43*(8), 1–15. https://doi.org/10.1111/jfpe.13448

Keneni, Y. G., Hvoslef-Eide, A. K. T., & Marchetti, J. M. (2019). Mathematical modelling of the drying kinetics of Jatropha curcas L. seeds. *Industrial Crops and Products, 132* (February), 12–20. https://doi.org/10.1016/j.indcrop.2019.02.012

Krug, R. R., Hunter, W. G., & Grieger, R. A. (1976a). Enthalpy-entropy compensation. 1. Some fundamental statistical problems associated with the analysis of van't hoff and arrhenius data. *Journal of Physical Chemistry, 80*(21), 2335–2341. https://doi.org/10.1021/j100562a006

Krug, R. R., Hunter, W. G., & Grieger, R. A. (1976b). Enthalpy-entropy compensation. 2. Separation of the chemical from the statistical effect. *Journal of Physical Chemistry, 80*(21), 2341–2351. https://doi.org/10.1021/j100562a007

Kurozawa, L. E., de Oliveira, R. A., Hubinger, M. D., & Park, K. J. (2015). Thermodynamic properties of water desorption of papaya. *Journal of Food Processing and Preservation, 39*(6), 2412–2420. https://doi.org/10.1111/jfpp.12491

Labuza, T. (1963). Creation of moisture sorption isotherms for hygroscopic materials. Sorption isotherm methods. In *International symposium on humidity and moisture.* Washington: American Society of Heating, Refrigerating and Air Conditioning Engineers. May 20-23.

Leffler, J. E. (1955). The enthalpy-entropy relationshipg and its implications for organic chemistry. *Journal of Organic Chemistry, 20*, 1202–1231.

Li, M., Wen, X., Peng, Y., Wang, Y., Wang, K., & Ni, Y. (2018). Functional properties of protein isolates from bell pepper (Capsicum annuum L. var. annuum) seeds. *Lebensmittel-Wissenschaft & Technologie, 97*, 802–810. https://doi.org/10.1016/J.LWT.2018.07.069

López, D. N., Galante, M., Robson, M., Boeris, V., & Spelzini, D. (2018). Amaranth, quinoa and chia protein isolates: Physicochemical and structural properties. *International Journal of Biological Macromolecules, 109*, 152–159. https://doi.org/10.1016/J.IJBIOMAC.2017.12.080

Lozano, Y. F., Mayer, C. D., Bannon, C., & Gaydou, E. M. (1993). Unsaponifiable matter, total sterol and tocopherol contents of avocado oil varieties. *Journal of the American Oil Chemists' Society, 70*(6), 561–565. https://doi.org/10.1007/BF02545319

Lu, Z. X., He, J. F., Zhang, Y. C., & Bing, D. J. (2019). *Composition, physicochemical properties of pea protein and its application in functional foods, 60* pp. 2593–2605). https://doi.org/10.1080/10408398.2019.1651248, 15.

Ma, Y., Wu, X., Zhao, L., Wang, Y., & Liao, X. (2019a). Comparison of the compounds and characteristics of pepper seed oil by pressure-assisted, ultrasound-assisted and conventional solvent extraction. *Innovative Food Science & Emerging Technologies, 54*, 78–86. https://doi.org/10.1016/J.IFSET.2019.03.011

Ma, Y., Wu, X., Zhao, L., Wang, Y., & Liao, X. (2019b). Comparison of the compounds and characteristics of pepper seed oil by pressure-assisted, ultrasound-assisted and conventional solvent extraction. *Innovative Food Science & Emerging Technologies, 54*, 78–86. https://doi.org/10.1016/J.IFSET.2019.03.011

Mallek-Ayadi, S., Bahloul, N., & Kechaou, N. (2020). Mathematical modelling of water sorption isotherms and thermodynamic properties of Cucumis melo L. seeds. *Lwt, 131*(June), Article 109727. https://doi.org/10.1016/j.lwt.2020.109727

Martins, M. J. N., Sanches, M. A. R., Polachini, T. C., Oliveira, E. B., Coimbra, J. S. R., & Telis-Romero, J. (2023). Solubility of different salts used in the control of the water activity of foods. *Science and Agrotechnology, 47*, Article e018722. https://doi.org/10.1590/1413-7054202347018722

Mattila, P., Mäkinen, S., Eurola, M., Jalava, T., Pihlava, J.-M., Hellström, J., & Pihlanto, A. (2018). Nutritional value of commercial protein-rich plant products. *Plant Foods for Human Nutrition, 73*(2), 108–115. https://doi.org/10.1007/s11130-018-0660-7

AOCS. (2009). In V. C. Mehlenbacher, & I. L. Urbana (Eds.) (6th ed.)*American oil chemists' societyOfficial methods and recommended practices of the American oil chemists' society*.

Moreno-Escamilla, J. O., de la Rosa, L. A., López-Díaz, J. A., Rodrigo-García, J., Núñez-Gastélum, J. A., & Alvarez-Parrilla, E. (2015). Effect of the smoking process and firewood type in the phytochemical content and antioxidant capacity of red Jalapeño pepper during its transformation to chipotle pepper. *Food Research International, 76*, 654–660. https://doi.org/10.1016/J.FOODRES.2015.07.031

Nicoleti, J. F., Telis-Romero, J., & Telis, V. R. N. (2007). *Air-drying of fresh and osmotically pre-treated pineapple slices: Fixed air temperature versus fixed slice temperature drying kinetics, 19* pp. 2175–2191). https://doi.org/10.1081/DRT-100107493, 9.

Nip, W. K. (2005). Manufacture of fermented product. In *Handbook of food science, technology, and engineering, 4* pp. 3131–3154). https://doi.org/10.1201/B15995-203

O'Brien, R. D. (2009). *Fats and oils: Formulating and processing for applications* (3rd ed.). CRC Press. https://doi.org/10.1201/9781420061673

Perea-Flores, M. J., Garibay-Febles, V., Chanona-Pérez, J. J., Calderón-Domínguez, G., Méndez-Méndez, J. V., Palacios-González, E., & Gutiérrez-López, G. F. (2012). Mathematical modelling of castor oil seeds (Ricinus communis) drying kinetics in fluidized bed at high temperatures. *Industrial Crops and Products, 38*(1), 64–71. https://doi.org/10.1016/j.indcrop.2012.01.008

Polachini, T. C., Betiol, L. F. L., Lopes-Filho, J. F., & Telis-Romero, J. (2016). Water adsorption isotherms and thermodynamic properties of cassava bagasse. *Thermochimica Acta, 632*, 79–85. https://doi.org/10.1016/j.tca.2016.03.032

Rezazadeh, A., Moghaddas Kia, E., Hamishehkar, H., Kafil Gazi Jahani, B., & Ghasempour, Z. (2022). Capsaicin-incorporated zein electrospun nanofibers: Characterization and release behavior. *Food Bioscience, 49*, Article 101843. https://doi.org/10.1016/J.FBIO.2022.101843

Rizvi, S. S. H. (2014). Thermodynamic properties of foods in dehydration. In M. A. Rao, S. S. H. Rizvi, & A. K. Datta (Eds.), *Engineering properties of foods* (4th ed., pp. 359–436). CRC Press.

Rosa, D. P., Cantú-Lozano, D., Luna-Solano, G., Polachini, T. C., & Telis-Romero, J. (2015). Modelagem matemática da cinética de secagem de semente de laranja. *Ciencia E Agrotecnologia, 39*(3), 291–300. https://doi.org/10.1590/S1413-70542015000300011

Rosa, D. P., Evangelista, R. R., Borges Machado, A. L., Sanches, M. A. R., & Telis-Romero, J. (2021). Water sorption properties of papaya seeds (Carica papaya L.) formosa variety: An assessment under storage and drying conditions. *Lwt, 138*. https://doi.org/10.1016/j.lwt.2020.110458 (June 2020).

Sá, A. G. A., Moreno, Y. M. F., & Carciofi, B. A. M. (2020). Plant proteins as high-quality nutritional source for human diet. *Trends in Food Science & Technology, 97*, 170–184. https://doi.org/10.1016/J.TIFS.2020.01.011

Sandoval-Castro, C. J., Valdez-Morales, M., Oomah, B. D., Gutiérrez-Dorado, R., Medina-Godoy, S., & Espinosa-Alonso, L. G. (2017). Bioactive compounds and antioxidant activity in scalded Jalapeño pepper industrial byproduct (Capsicum annuum). *Journal of Food Science and Technology, 54*(7), 1999–2010. https://doi.org/10.1007/s13197-017-2636-2

Sandoval-Castro, C. J., Valdez-Morales, M., Perea-Domínguez, X. P., Medina-Godoy, S., & Espinosa-Alonso, L. G. (2014). Antioxidant activity of processed and raw seed byproduct from Jalapeño pepper. *J Chem Biol Phys Sci Spec, 4*(5). Journal of Chemical Biological and Physical Science, 4(5).

Sangroula, G., Khatri, S. B., Sangroula, P., Basnet, A., Khadka, N., & Khadka, M. (2024). Essential oil of black pepper (Piper nigrum) and cardamom (Amomum sublatum roxb) as a natural food preservative for plum RTS. *Journal of Agriculture and Food Research, 16*, Article 101159. https://doi.org/10.1016/J.JAFR.2024.101159

Schwarz, G. (1978). Estimating the dimension of a model. *Annals of Statistics, 6*(2), 461–464. https://doi.org/10.1214/aos/1176344136

Sharma, S. K., Vij, A. S., & Sharma, M. (2013). Mechanisms and clinical uses of capsaicin. *European Journal of Pharmacology, 720*(1–3), 55–62. https://doi.org/10.1016/J.EJPHAR.2013.10.053

Silva, K. S., Polachini, T. C., Luna-Flores, M., Luna-Solano, G., Resende, O., & Telis-Romero, J. (2021). Sorption isotherms and thermodynamic properties of wheat malt under storage conditions. *Journal of Food Process Engineering, 44*(9), 1–12. https://doi.org/10.1111/jfpe.13784

Singleton, V. L., Orthofer, R., & Lamuela-Raventós, R. M. (1999). [14] Analysis of total phenols and other oxidation substrates and antioxidants by means of folin-ciocalteu reagent. *Methods in Enzymology, 299*, 152–178. https://doi.org/10.1016/S0076-6879(99)99017-1

Sora, G. T. S., Haminiuk, C. W. I., da Silva, M. V., Zielinski, A. A. F., Gonçalves, G. A., Bracht, A., & Peralta, R. M. (2015). A comparative study of the capsaicinoid and phenolic contents and in vitro antioxidant activities of the peppers of the genus Capsicum: An application of chemometrics. *Journal of Food Science and Technology, 52*(12), 8086–8094. https://doi.org/10.1007/S13197-015-1935-8/TABLES/3

Spada, J. C., Noreña, C. P. Z., Marczak, L. D. F., & Tessaro, I. C. (2013). Water adsorption isotherms of microcapsules with hydrolyzed pinhão (Araucaria angustifolia seeds) starch as wall material. *Journal of Food Engineering, 114*(1), 64–69. https://doi.org/10.1016/j.jfoodeng.2012.07.019

Spiess, W. E. L., & Wolf, W. F. (1983). The results of the COST 90 project on water activity. In R. Jowitt (Ed.), *Physical properties of foods* (pp. 65–91). Applied Science Publishers.

Tagnamas, Z., Bahammou, Y., Moussaoui, H., Kouhila, M., Lamsyehe, H., Idlimam, A., & Lamharrar, A. (2021). Exploring the sorption and thermodynamic proprieties of white truffle (Terfezia boudieri). *Journal of Food Process Engineering, 44*(12), 1–11. https://doi.org/10.1111/jfpe.13888

Tavakoli, J., Emadi, T., Hashemi, S. M. B., Mousavi Khaneghah, A., Munekata, P. E. S., Lorenzo, J. M., Brnčić, M., & Barba, F. J. (2018). Chemical properties and oxidative stability of Arjan (Amygdalus reuteri) kernel oil as emerging edible oil. *Food Research International, 107*(February), 378–384. https://doi.org/10.1016/j.foodres.2018.02.002

Valdez-Morales, M., Sandoval-Castro, C. J., Gutiérrez-Dorado, R., Mendoza-Espinoza, J. A., Medina-Godoy, S., & Espinosa-Alonso, L. G. (2021). Oil recovery from jalapeño pepper by-products and analysis of the industrial scalding process on its nutraceutical potential. *Waste and Biomass Valorization, 12*(8), 4475–4487. https://doi.org/10.1007/S12649-020-01323-8/TABLES/4

Vega-Gálvez, A., Miranda, M., Díaz, L. P., Lopez, L., Rodriguez, K., & Scala, K. Di (2010). Effective moisture diffusivity determination and mathematical modelling of the drying curves of the olive-waste cake. *Bioresource Technology, 101*(19), 7265–7270. https://doi.org/10.1016/J.BIORTECH.2010.04.040

Wagenmakers, E.-J., & Farrell, S. (2004). AIC model selection using Akaike weights. *Psychonomic Bulletin & Review, 11*(1), 192–196. https://doi.org/10.3758/BF03206482

Wolfinger, R. (1993). Covariance structure selection in general mixed models. *Communications in Statistics - Simulation and Computation, 22*(4), 1079–1106. https://doi.org/10.1080/03610919308813143

Xie, Y., Lin, Y., Li, X., Yang, H., Han, J., Shang, C., Li, A., Xiao, H., & Lu, F. (2022). Peanut drying: Effects of various drying methods on drying kinetic models, physicochemical properties, germination characteristics, and microstructure. *Information Processing in Agriculture, 10*(4), 447–458. https://doi.org/10.1016/j.inpa.2022.04.004

Yogendrarajah, P., Samapundo, S., Devlieghere, F., De Saeger, S., & De Meulenaer, B. (2015). Moisture sorption isotherms and thermodynamic properties of whole black peppercorns (Piper nigrum L.). *Lwt, 64*(1), 177–188. https://doi.org/10.1016/j.lwt.2015.05.045

Zhang, D., Huang, D., Zhang, X., Zhao, H., Gong, G., Tang, X., & Li, L. (2023). Drying performance and energy consumption of Camellia oleifera seeds under microwave-vacuum drying. *Food Science and Biotechnology, 32*(7), 969–977. https://doi.org/10.1007/s10068-022-01239-0

Zhang, Z. shan, Li, X. dan, Jia, H. jie, & Liu, Y. lan (2022). Moisture sorption isotherms and thermodynamic properties of tiger nuts: An oil-rich tuber. *Lwt, 167*(100), Article 113866. https://doi.org/10.1016/j.lwt.2022.113866

Zhao, D., Wei, J., Hao, J., Han, X., Ding, S., Yang, L., & Zhang, Z. (2019). Effect of sodium carbonate solution pretreatment on drying kinetics, antioxidant capacity changes, and final quality of wolfberry (Lycium barbarum) during drying. *Lebensmittel-Wissenschaft & Technologie, 99*, 254–261. https://doi.org/10.1016/j.lwt.2018.09.066

Zhishen, J., Mengcheng, T., & Jianming, W. (1999). The determination of flavonoid contents in mulberry and their scavenging effects on superoxide radicals. *Food Chemistry, 64*(4), 555–559. https://doi.org/10.1016/S0308-8146(98)00102-2